Science Advances
AAAS

advances.sciencemag.org/cgi/content/full/5/6/eaax2348/DC1

# Supplementary Materials for

## Solvent-dependent segmental dynamics in intrinsically disordered proteins

Nicola Salvi*, Anton Abyzov, Martin Blackledge*

*Corresponding author. Email: nicola.salvi@ibs.fr (N.S.); martin.blackledge@ibs.fr (M.B.)

Published 28 June 2019, *Sci. Adv.* **5**, eaax2348 (2019)
DOI: 10.1126/sciadv.aax2348

**This PDF file includes:**

Reference (*61*)

**Table S1. Summary of the MD simulations carried out on the C-terminal domain of Sendai virus and discussed in the present work.** Simulations **A4P_25** and **C3P_25** were presented in references (28) and (30).

| | trajectories | ns/trajectory | total sim. time (μs) | ns/segment | segments/traj | segments |
|---|---|---|---|---|---|---|
| **C36m/TIP3P, 25°C (C3P@25C)** | 24 | 200 | 4.8 | 100 | 3 | 72 |
| **C36m/TIP3P, 15°C (C3P@15C)** | 22 | 300 | 6.6 | 200 | 2 | 44 |
| **C36m/TIP3P, 5°C (C3P@5C)** | 22 | 400 | 8.8 | 300 | 2 | 44 |
| **C36m/TIP4P/2005, 25°C (C4P@25C)** | 21 | 200 | 4.2 | 100 | 3 | 63 |
| **C36m/TIP4P/2005, 15°C (C4P@15C)** | 20 | 300 | 6.0 | 200 | 2 | 40 |
| **C36m/TIP4P/2005, 5°C (C4P@5C)** | 28 | 400 | 11.2 | 300 | 2 | 56 |
| **A99SB-ILDN/TIP4P/2005, 25°C (A4P@25C)** | 10 | 250 | 2.5 | 100 | 4 | 40 |
| **A99SB-ILDN/TIP4P/2005, 15°C (A4P@15C)** | 25 | 300 | 7.5 | 200 | 2 | 50 |
| **A99SB-ILDN/TIP4P/2005, 5°C (A4P@5C)** | 21 | 400 | 8.4 | 300 | 2 | 42 |
| total | **193** | | 60.0 | | | **451** |

**Table S2. Summary of the results of the ABSURD procedure.**

| | Relaxation rate used for the selection | $\chi^2_{ABSURD}/\chi^2_{average}$ | Number of selected segments |
|---|---|---|---|
| **C36m/TIP3P, 25°C (C3P@25C)** | $^{15}N\{^1H\}$ NOE at 600 MHz (5) | 0.246 | 17 |
| **C36m/TIP3P, 15°C (C3P@15C)** | $\eta_{xy}$ at 850 MHz | 0.402 | 10 |
| **C36m/TIP3P, 5°C (C3P@5C)** | $\eta_{xy}$ at 600 MHz | 0.397 | 6 |
| **C36m/TIP4P/2005, 25°C (C4P@25C)** | $^{15}N$ $R_2$ at 950 MHz | 0.123 | 10 |
| **C36m/TIP4P/2005, 15°C (C4P@15C)** | $\eta_{xy}$ at 850 MHz | 0.133 | 7 |
| **C36m/TIP4P/2005, 5°C (C4P@5C)** | $^{15}N$ $R_2$ at 850 MHz | 0.048 | 6 |
| **A99SB-ILDN/TIP4P/2005, 25°C (A4P@25C)** | $^{15}N$ $R_2$ at 950 MHz (6) | 0.160 | 6 |
| **A99SB-ILDN/TIP4P/2005, 15°C (A4P@15C)** | $^{15}N$ $R_2$ at 700 MHz | 0.133 | 5 |
| **A99SB-ILDN/TIP4P/2005, 5°C (A4P@5C)** | $\eta_{xy}$ at 600 MHz | 0.072 | 5 |

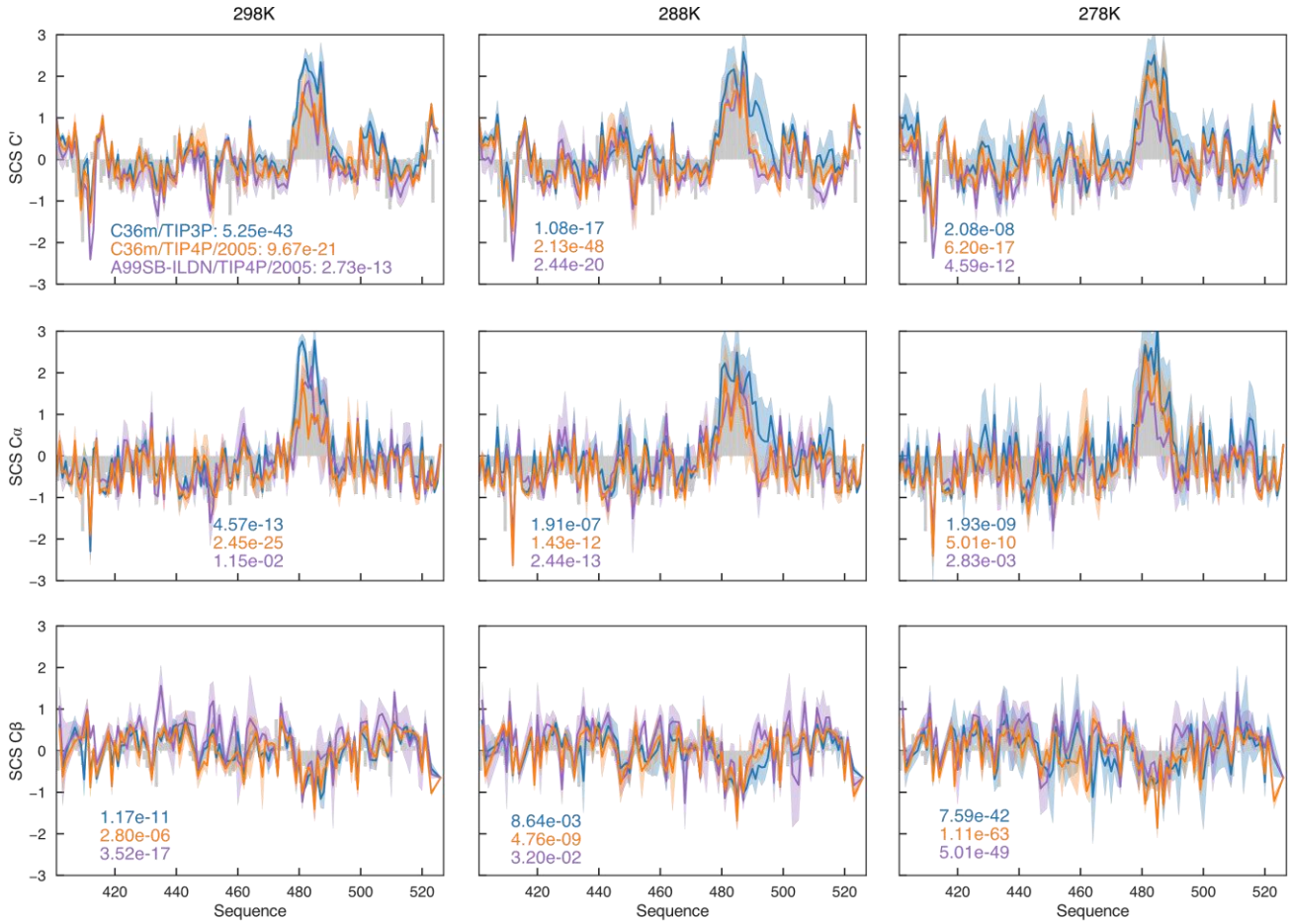


**Fig. S1. Experimental secondary chemical shifts (bars) compared with values calculated using frames extracted from the trajectories every 500 ps as input to SPARTA+** (61). Blue, orange and purple lines correspond to simulations **C3P**, **C4P** and **A4P**, respectively. p-values corresponding to the three simulation are shown in the panels. Notice that simulated values at 25 (left), 15 (middle) and 5 °C (right) are all compared to experimental values measured at 25 °C. $^{13}C$ chemical shifts in $N_{tail}$ change modestly with temperature (29).

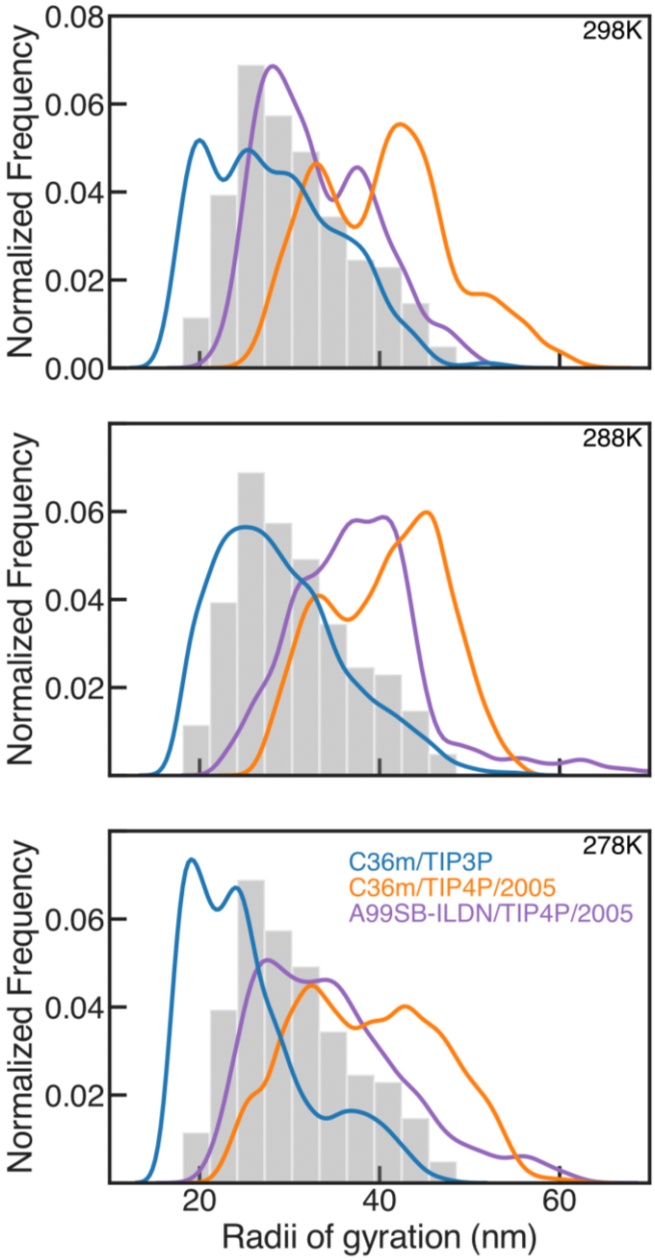


**Fig. S2. Distribution of radii of gyration in the ensemble used to seed the MD simulations (bars) compared with those calculated using frames extracted from the trajectories every 200 ps.** Blue, orange and purple lines correspond to simulations **C3P**, **C4P** and **A4P**, respectively.

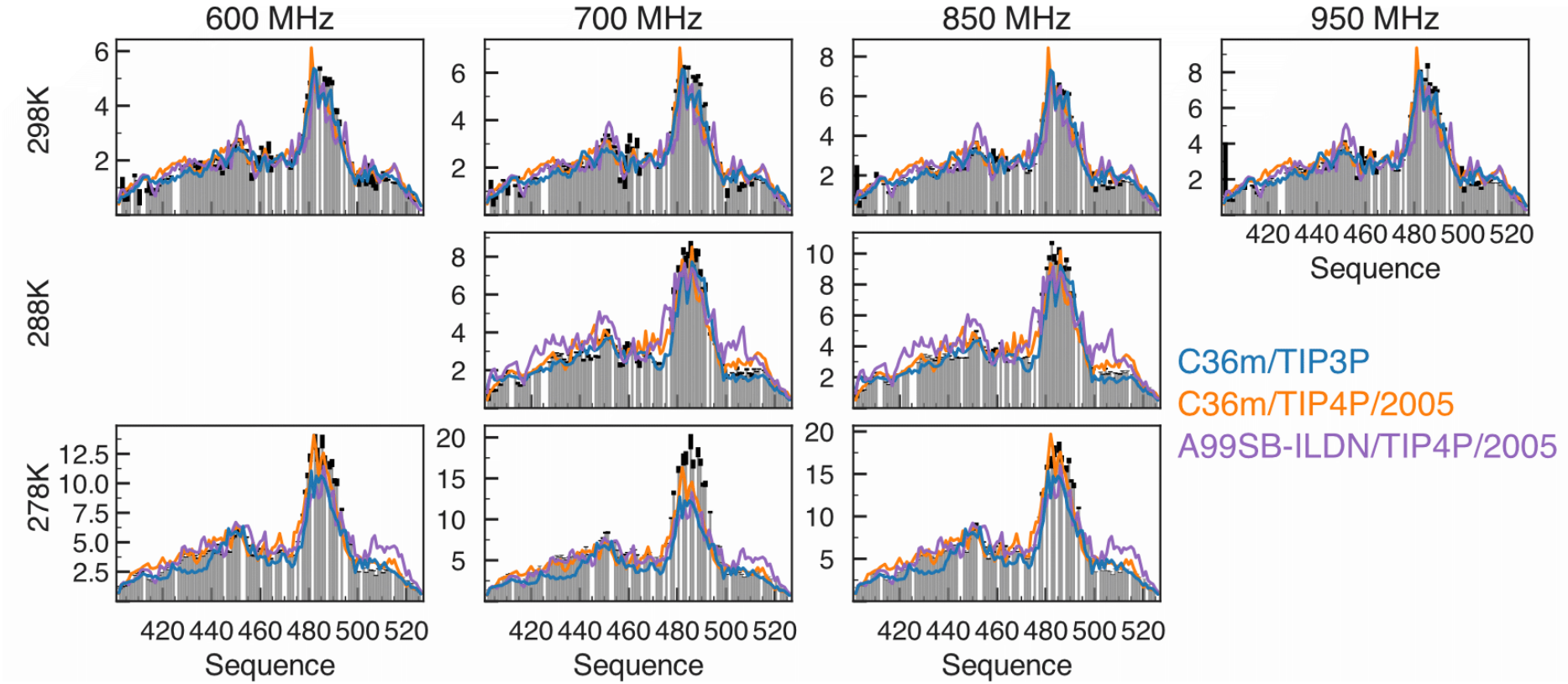


**Fig. S3. Experimental $^{15}$N chemical shift anisotropy/dipole-dipole cross-correlated cross-relaxation rates ($\eta_{xy}$) measured on $N_{tail}$ compared with the results of simulations.** All simulations - **C3P** (blue line), **C4P** (orange), and **A4P** (purple) - reproduce, at least qualitatively, the sequence dependence of $R_2$ rates. However, we notice that simulations are more accurate at room temperature than at lower T. All rates are reported in $s^{-1}$

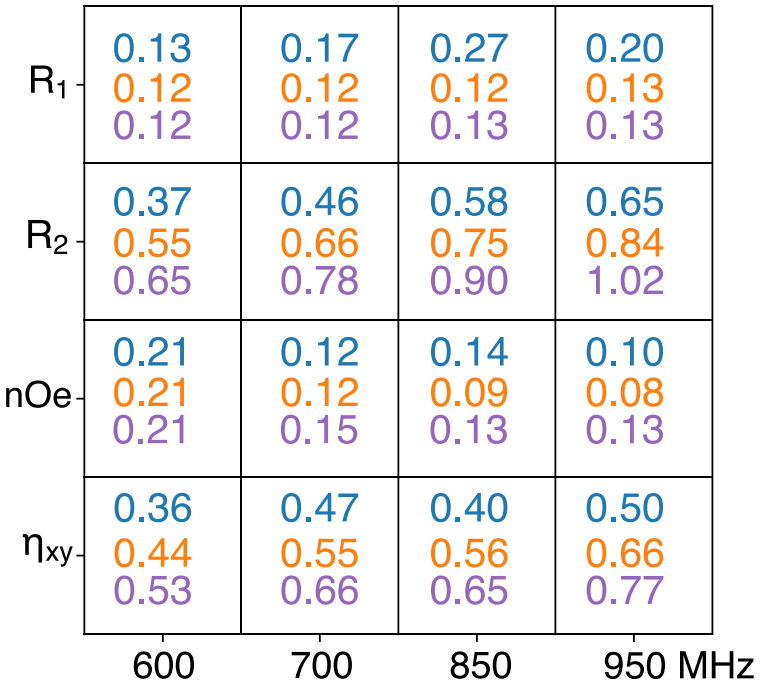


**Fig. S4. Root-mean-square deviations between experimental and simulated spin relaxation rates at 298K.** Values calculated using simulations **C3P**, **C4P**, and **A4P** are shown in blue, orange and purple, selectively

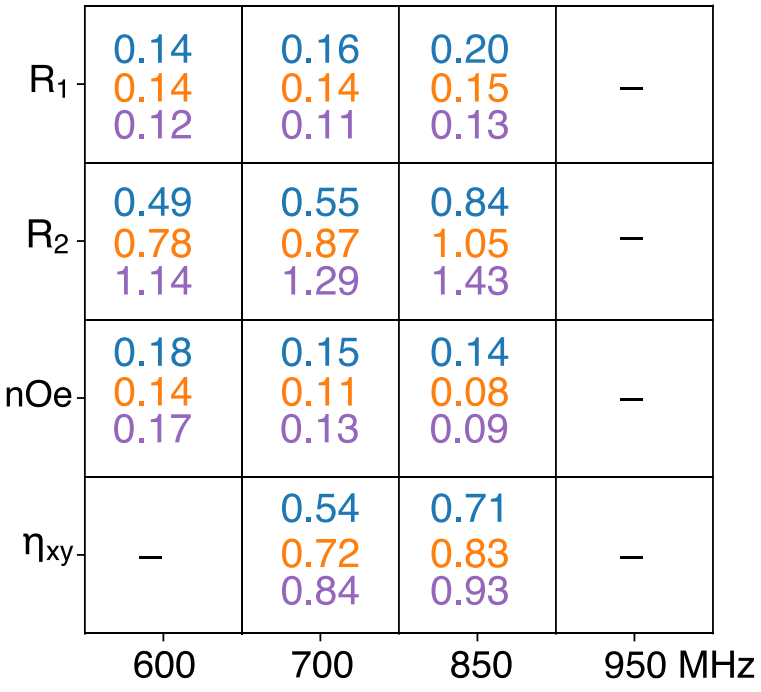


**Fig. S5. Root-mean-square deviations between experimental and simulated spin relaxation rates at 288K.** Values calculated using simulations **C3P**, **C4P**, and **A4P** are shown in blue, orange and purple, selectively.

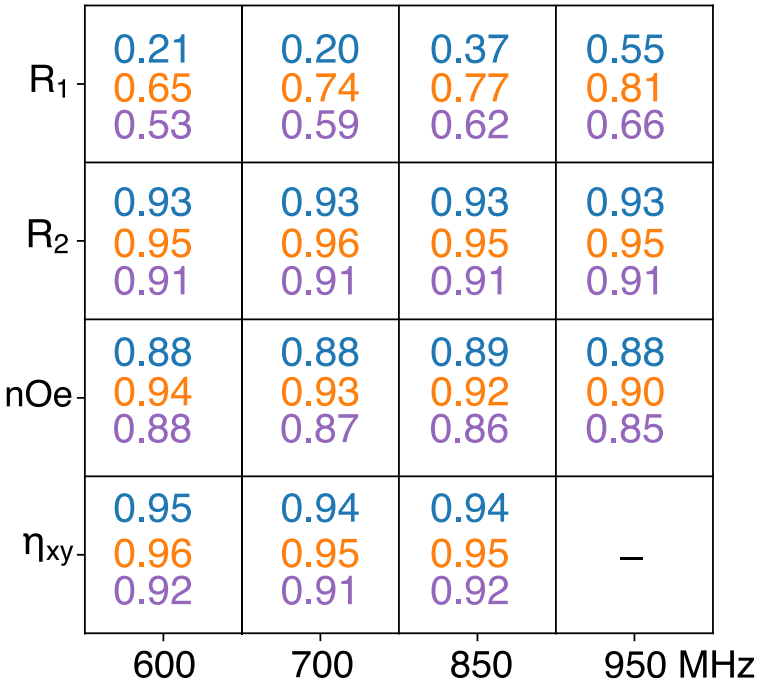


**Fig. S6. Root-mean-square deviations between experimental and simulated spin relaxation rates at 278K.** Values calculated using simulations **C3P**, **C4P**, and **A4P** are shown in blue, orange and purple, selectively.

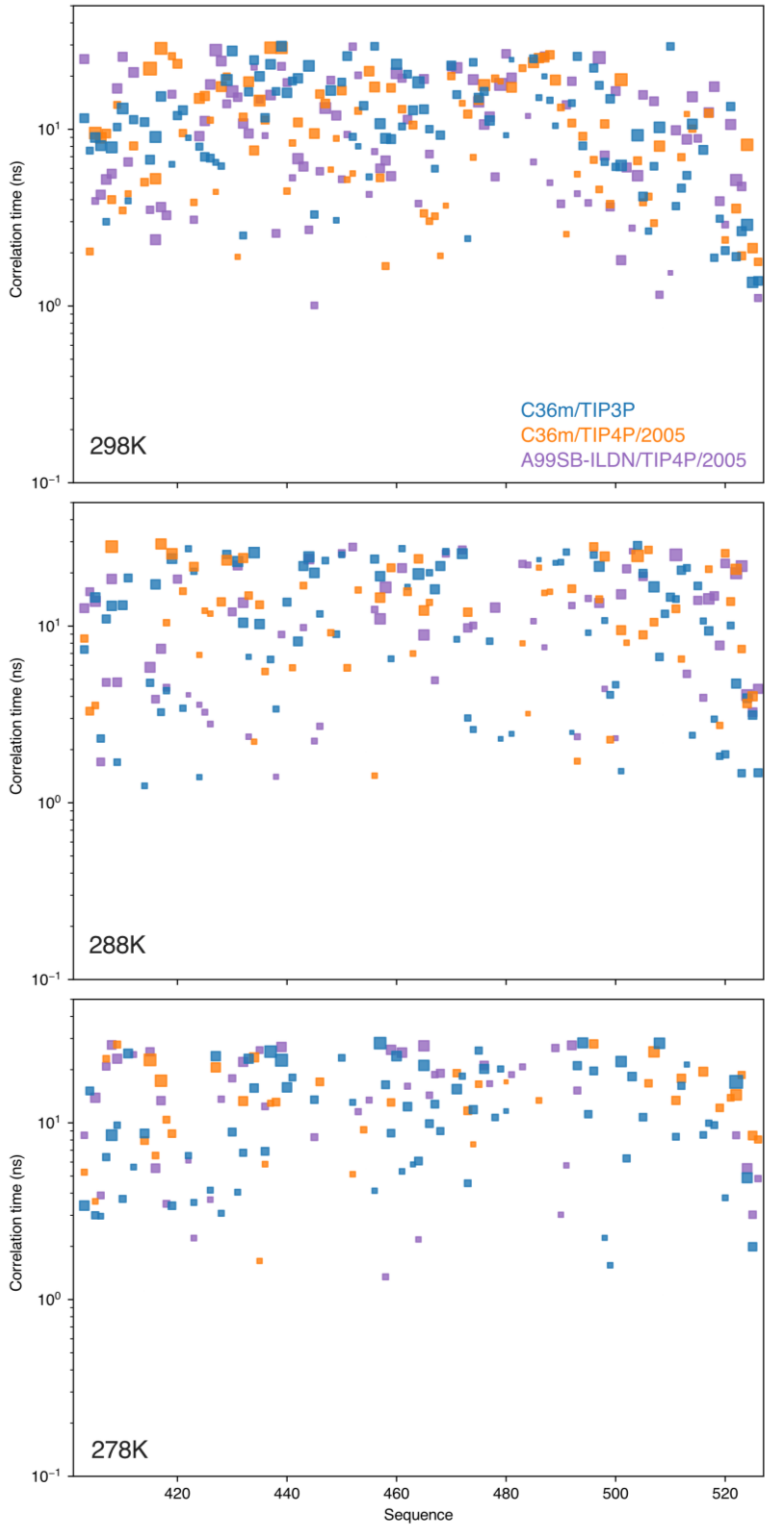


**Fig. S7. Time scales in the correlation function describing the contribution of backbone dihedral angles dynamics to relaxation of $^{15}$N backbone amide nuclei**. Symbol areas are proportional to the amplitude of the associated motional time scale at 298 (top), 288 (middle) and 278K (bottom).

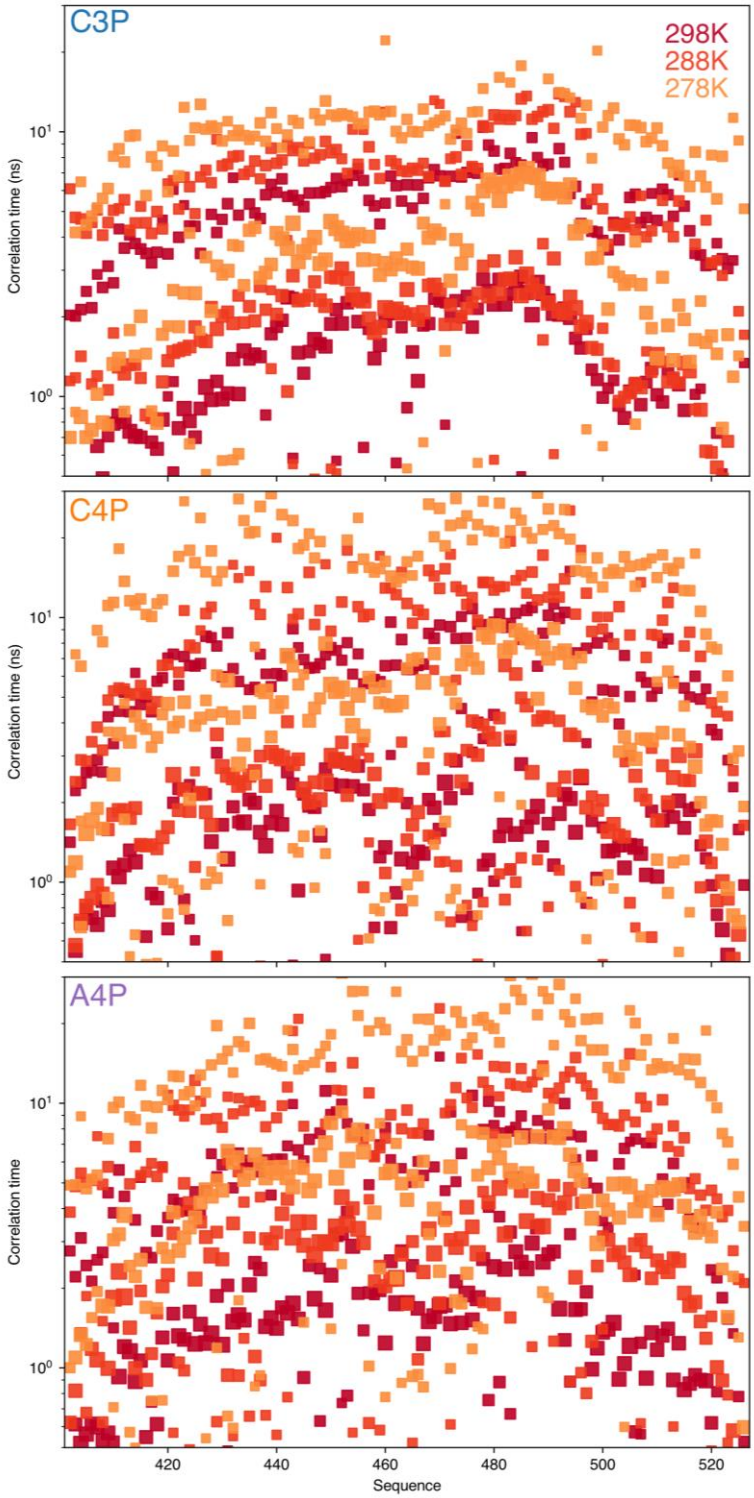


**Fig. S8. Time scales in the correlation function describing the contribution of segmental motions to relaxation of $^{15}$N backbone amide nuclei.** The size of the square is proportional to the amplitude of motions at the associated time scale in **C3P** (top), **C4P** (middle), and **A4P** (bottom).

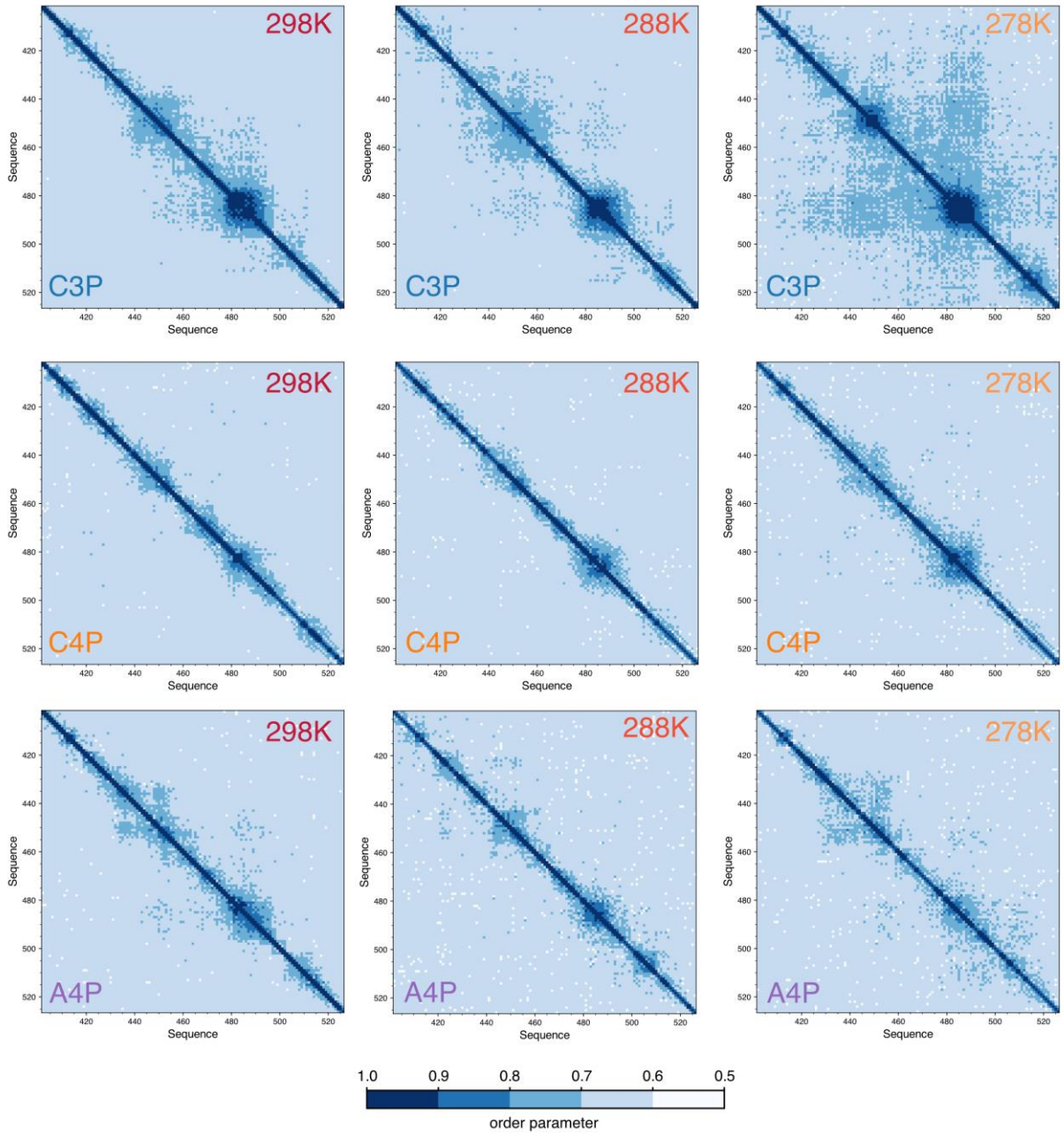


**Fig. S9. Fluctuations of the relative orientation of peptide planes measured by the order parameter $S^2_{seg}$.** The definition of order parameter is given in SI text. Order parameters are evaluated at different simulation temperatures and force field combinations. (top row: **C3P**; center: **C4P**; bottom row: **A4P**; left column: 298K; middle: 288K; right column: 278K).

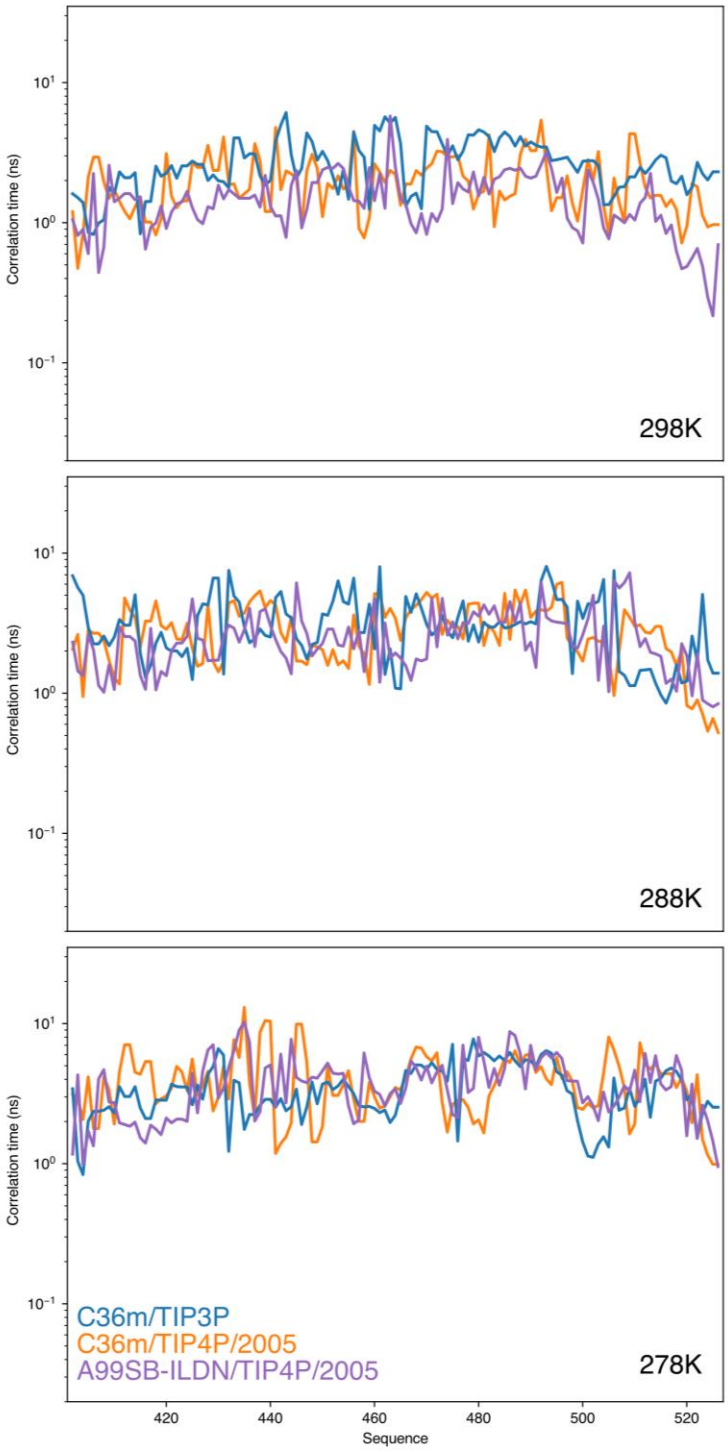


**Fig. S10. Time scales extracted from fits of correlation functions describing the rotational dynamics of segments to mono-exponential decays.** At all temperatures (top: 298K; middle: 288K; bottom: 278K) the three combination of protein/water force fields used in this paper produce equivalent descriptions of inter-segment dynamics.

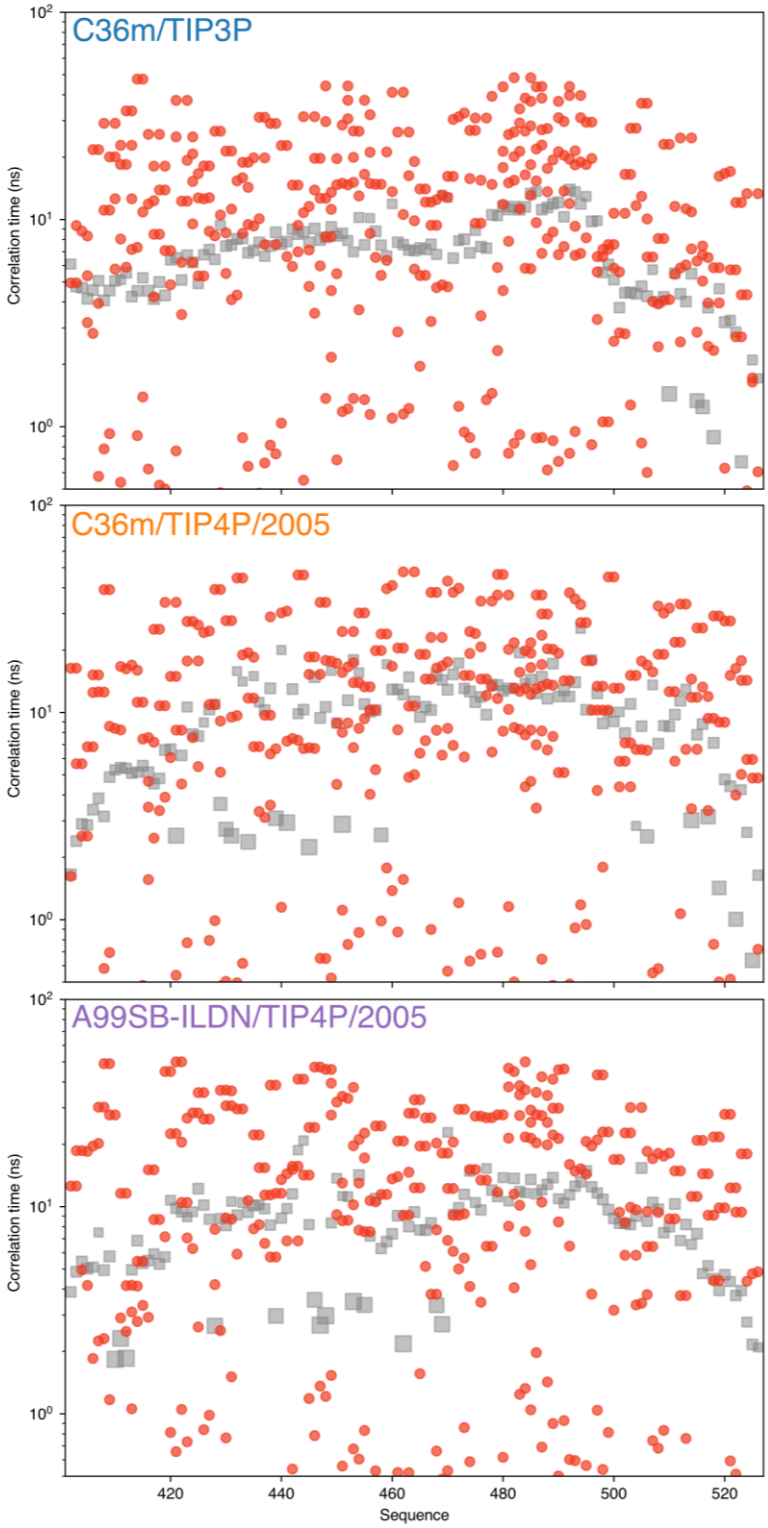


**Fig. S11. Time scales associated with intra-segment dynamics at 288K (orange circles) are compared with the longest timescale resulted from fitting segmental dynamics correlation functions (gray squares).** (top row: **C3P**; center: **C4P**; bottom row: **A4P**). See also fig. S8.

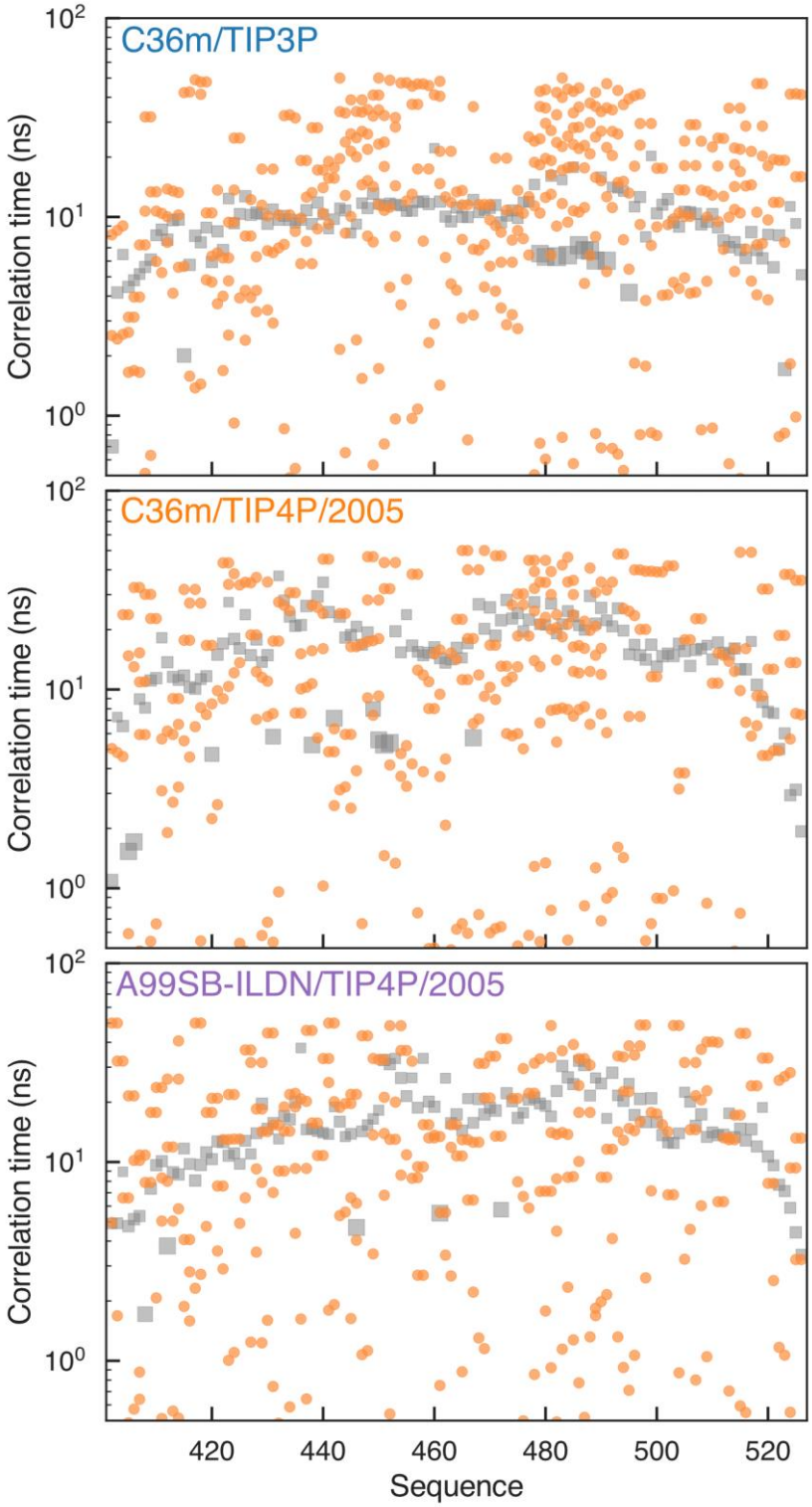


**Fig. S12. Time scales associated with intra-segment dynamics at 278K (yellow circles) are compared with the longest time scale resulted from fitting segmental dynamics correlation functions (gray squares).** (top row: **C3P**; center: **C4P**; bottom row: **A4P**). See also fig. S8.